Supporting Information for

Ambient Noise Tomography for a High-resolution 3D S-Wave Velocity Model of the Kinki Region, Southwestern Japan, using Dense Seismic Array Data

B. Nthaba[1,2], T. Ikeda[1,3], H. Nimiya[1,4], T. Tsuji[1,3], and Y. Iio[5]

[1] Department of Earth Resources Engineering, Kyushu University, Fukuoka, Japan,

[2] Earth and Environmental Sciences Department, Botswana International University of Science and Technology, P/Bag 16, Palapye, Botswana,

[3] International Institute for Carbon-Neutral Energy Research, Kyushu University, Fukuoka, Japan,

[4] Geological Survey of Japan, National Institute of Advanced Industrial Science and Technology (AIST), Ibaraki, Japan,

[5] Disaster Prevention Research Institute, Kyoto University, Kyoto, Japan.

Contents of this file

Figures S1 to S7

Introduction

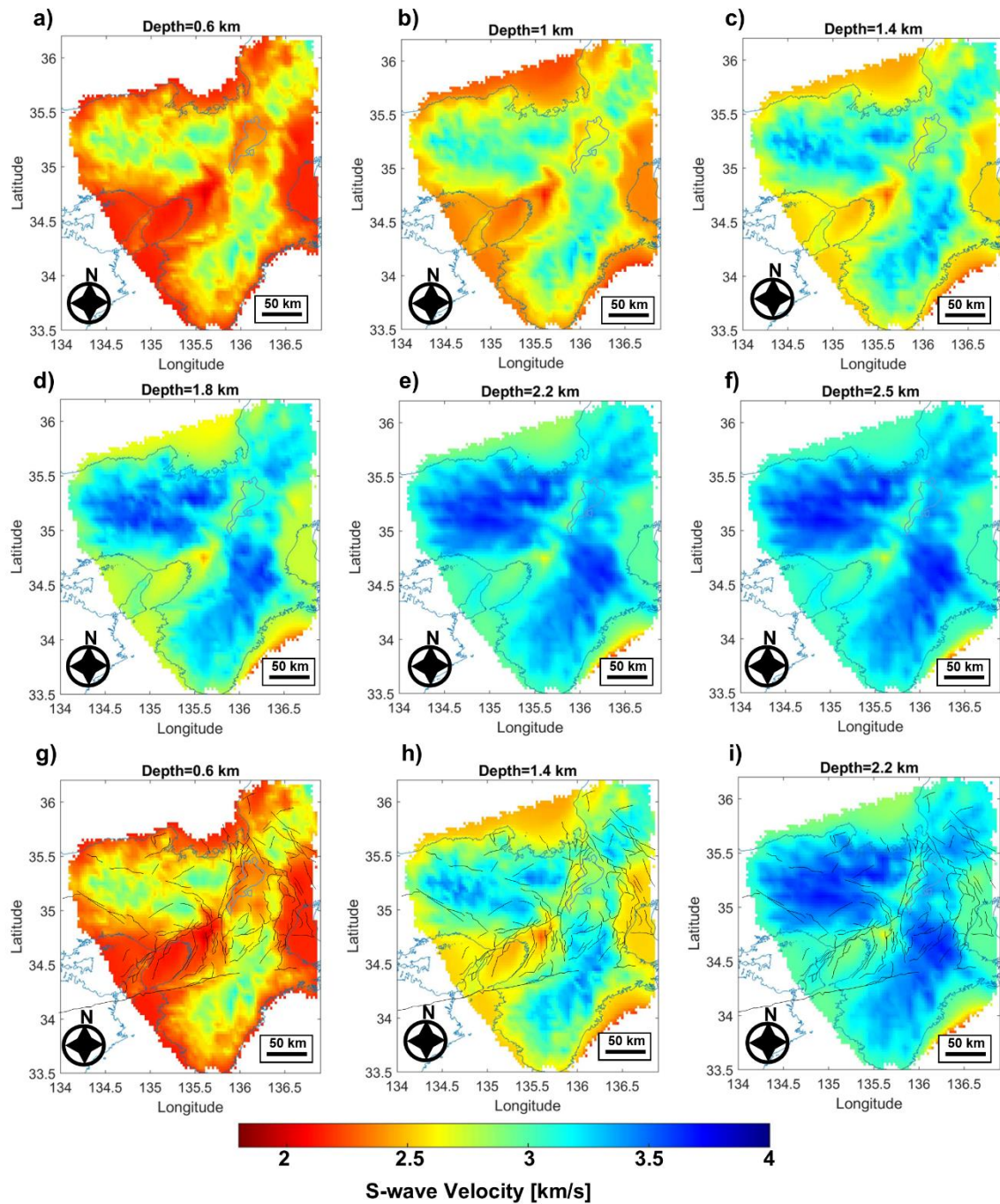Supplementary figures referred to in the main text are provided in this document.

Figure S1. Weakly smoothed S-wave velocity models at different depths below sea level, given above each panel. (a–f) S-wave velocity models without showing the active faults. (g–i) S-wave velocity models overlaid with active faults (black lines).
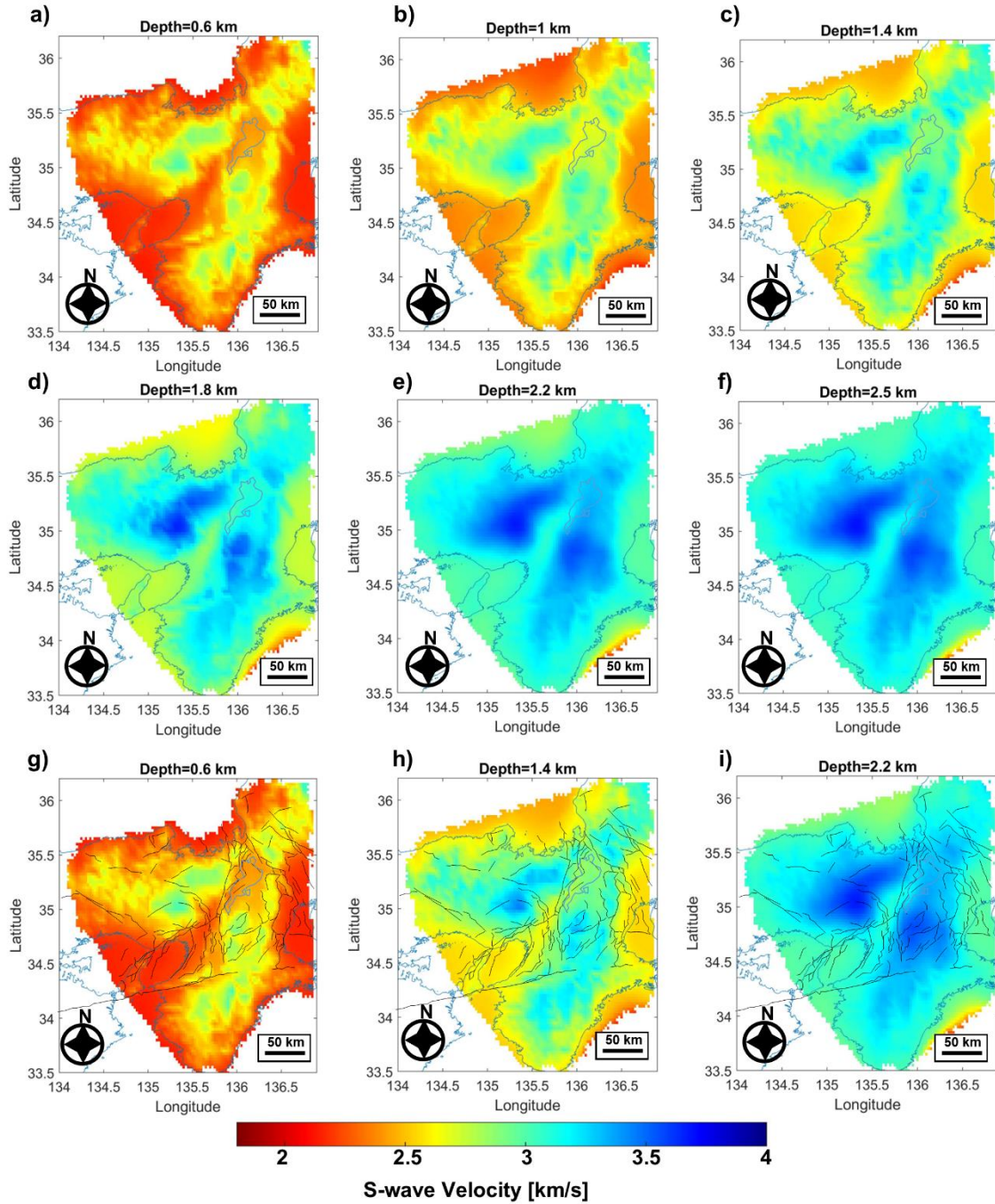
28

Figure S2. Strongly smoothed S-wave velocity models at different depths below sea
level, given above each panel. (a–f) S-wave velocity models without showing the active
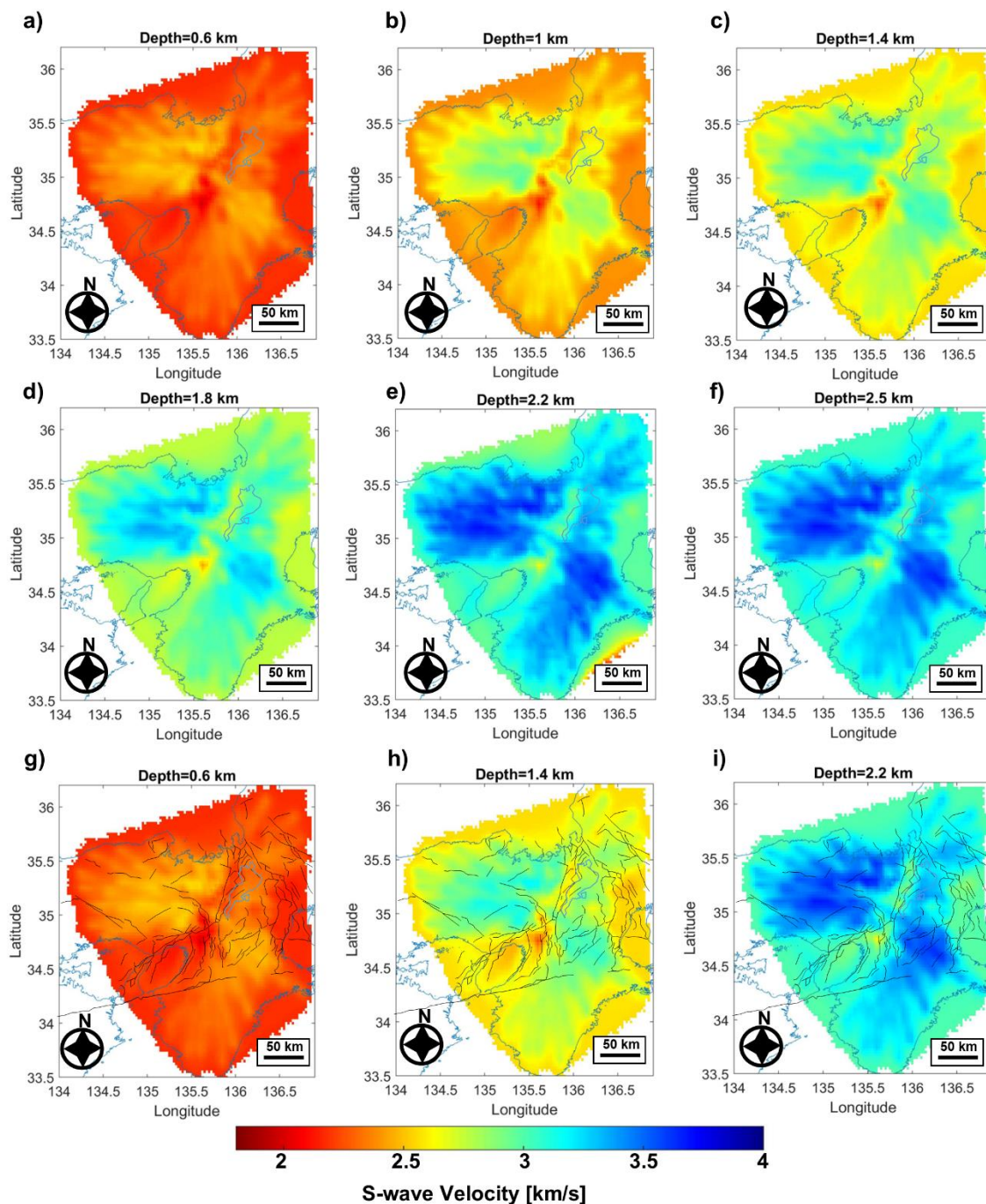faults. (g–i) S-wave velocity models overlaid with active faults (black lines).

Figure S3. Weakly smoothed S-wave velocity models at different depths before
topographic correction. (a–f) S-wave velocity models without showing the active faults.
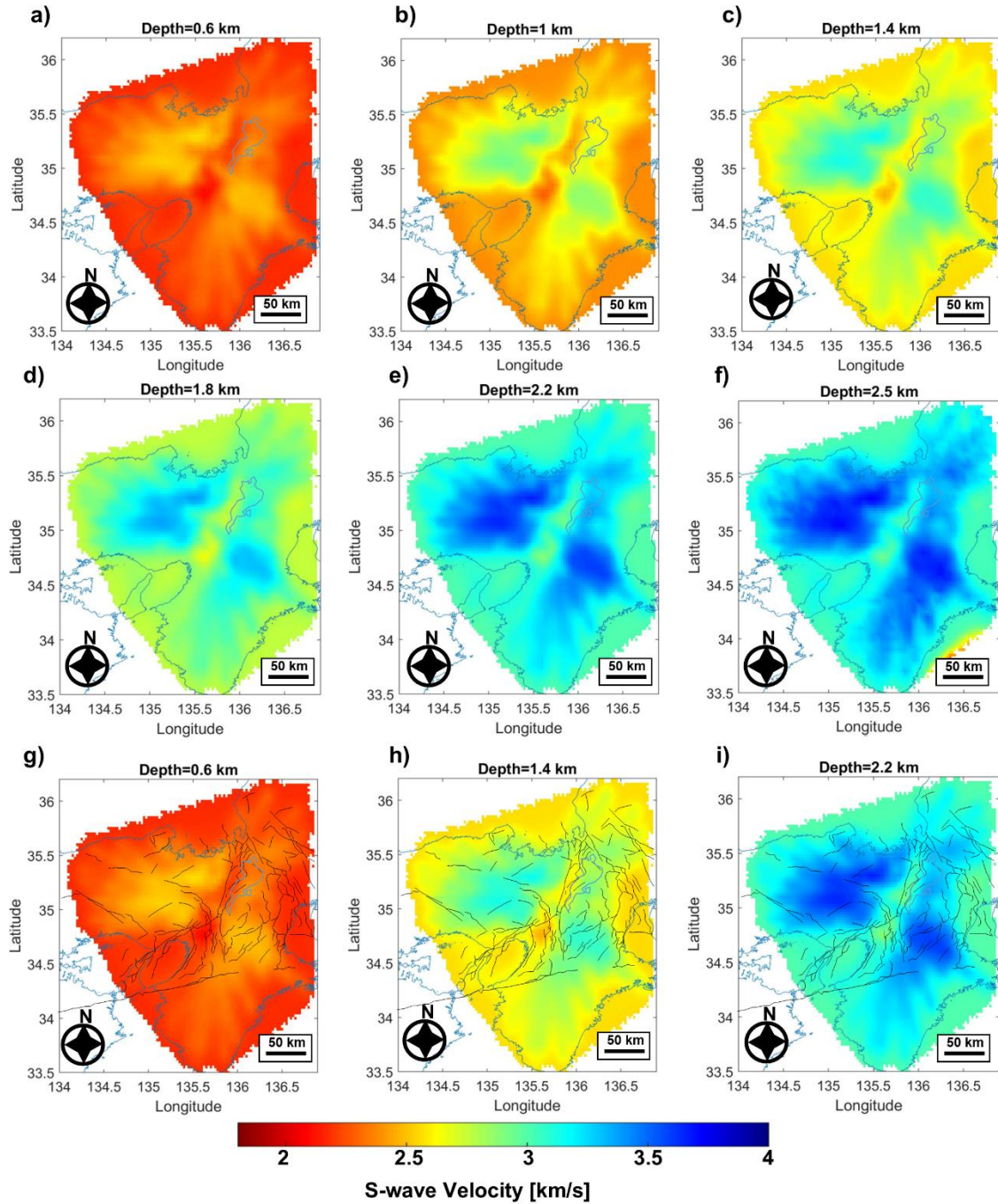(g–i) S-wave velocity models overlaid with active faults (black lines).

Figure S4. Moderately smoothed S-wave velocity models at different depths before topographic correction. (a–f) S-wave velocity models without showing the active faults. (g–i) S-wave velocity models overlaid with active faults (black lines).

43

Figure S5. Strongly smoothed S-wave velocity models at different depths before
topographic correction. (a–f) S-wave velocity models without showing the active faults.
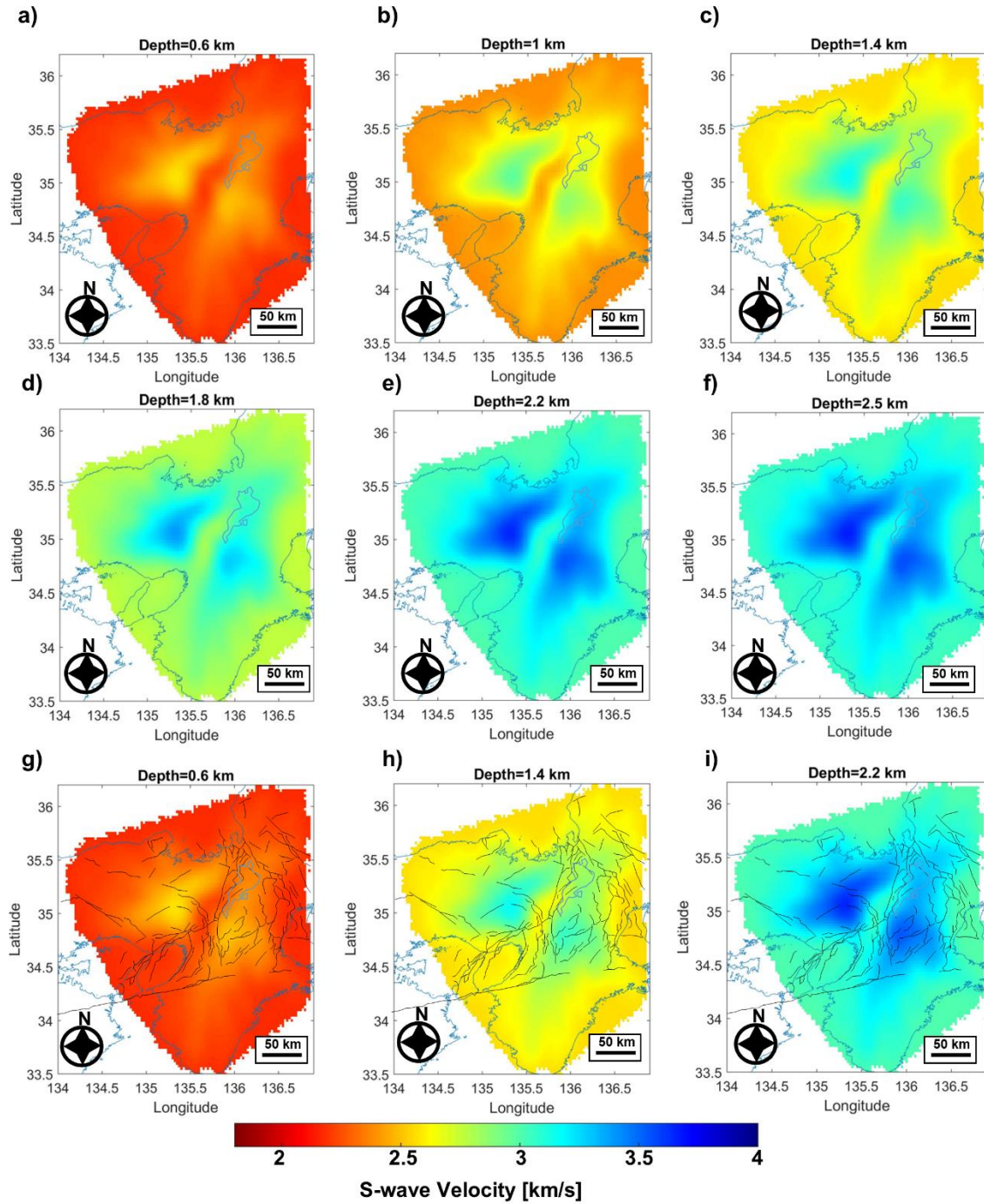(g–i) S-wave velocity models overlaid with active faults (black lines).
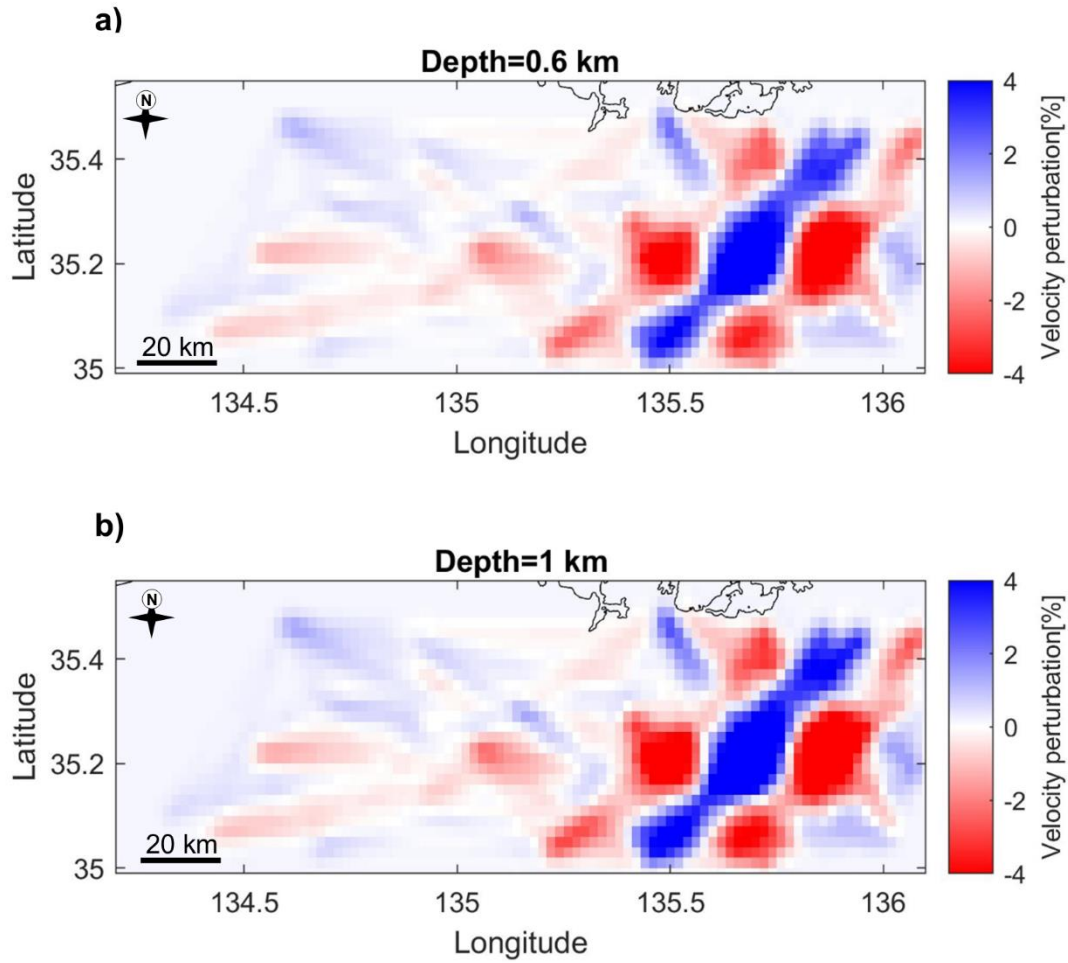
47

a)

Depth=0.6 km

b)

Depth=1 km

48

Figure S6. Horizontal velocity perturbation slices of the checkerboard resolution test results for the northern part of the Kinki region at 0.6 km (a) and 1 km (b) depths. The anomaly size was ~11 km (0.1°), and the velocity amplitude was ~10%. Depth is shown above each horizontal slice.
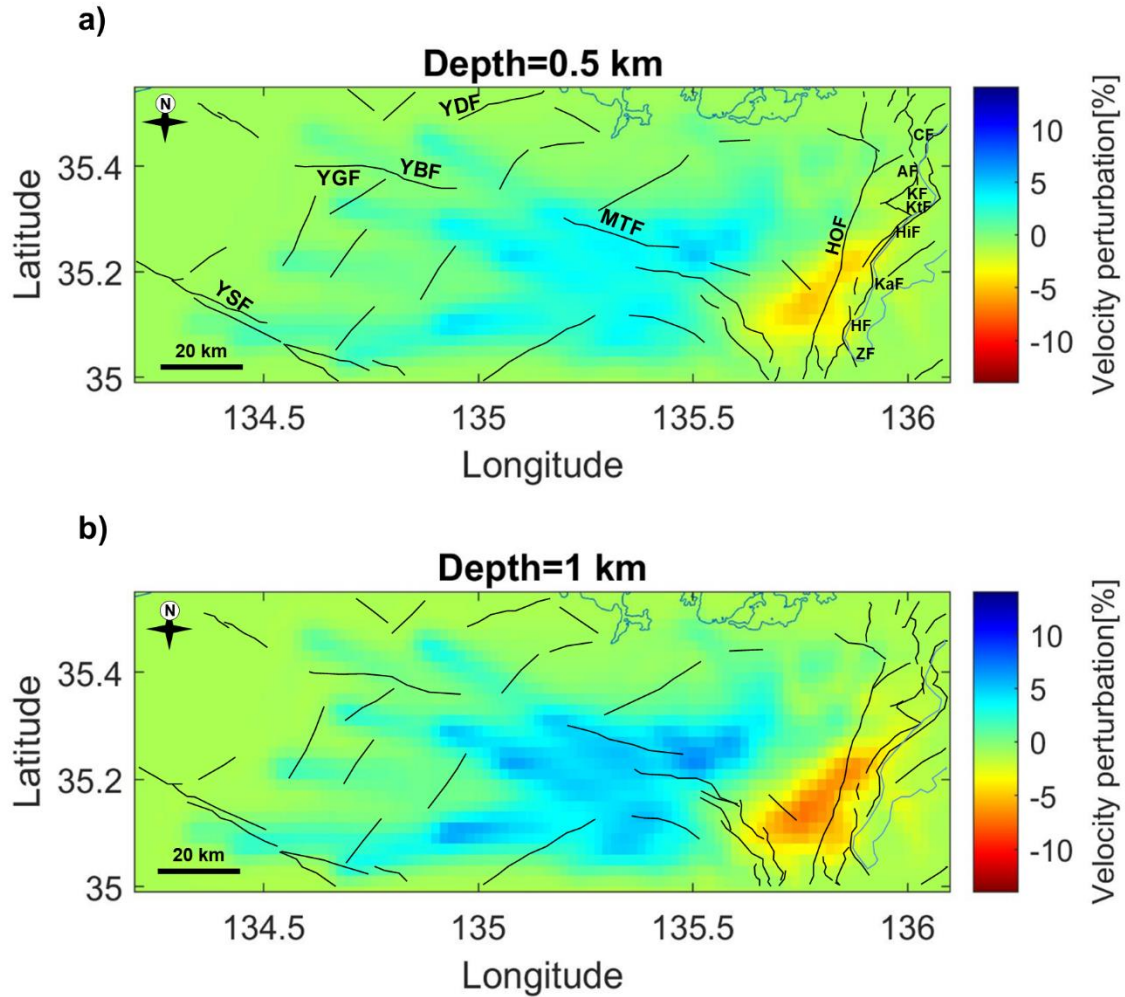
a)

b)

Figure S7. S-wave velocity perturbation of the northern part of the Kinki region before topographic correction. (a) S-wave velocity perturbation at a depth of 0.5 km below sea level. Also shown are the locations of the Yamada Fault (YDF), Yamasaki Fault (YSF), Yagi-Yabu Fault (YGF-YBF), Mitoke Fault (MTF), Hanaore Fault (HOF) and the Biwako-seigan Fault Zone members (Chinai Fault, CF; Aibano Fault, AF; Kamidera Fault, KF; Katsuno, KtF; Hira Fault, HiF; Katata, KaF; Hiei Fault, HF; Zeze Fault, ZF). (b) S-wave velocity perturbation at a depth of 1 km below sea level. Solid black lines represent documented active faults.